



HAL
open science

Diameter growth of boreal trees: Norwegian model applied to Finland

Kärenlampi Petri

► **To cite this version:**

Kärenlampi Petri. Diameter growth of boreal trees: Norwegian model applied to Finland. 2023. hal-04177282

HAL Id: hal-04177282

<https://hal.science/hal-04177282>

Preprint submitted on 4 Aug 2023

HAL is a multi-disciplinary open access archive for the deposit and dissemination of scientific research documents, whether they are published or not. The documents may come from teaching and research institutions in France or abroad, or from public or private research centers.

L'archive ouverte pluridisciplinaire **HAL**, est destinée au dépôt et à la diffusion de documents scientifiques de niveau recherche, publiés ou non, émanant des établissements d'enseignement et de recherche français ou étrangers, des laboratoires publics ou privés.

Diameter growth of boreal trees: Norwegian model applied to Finland

Kärenlampi Petri P.
Lehtoi Research, Lehtoi, Finland
petri.karenlampi@professori.fi

Abstract:

Norway Spruce growth in Central-South Finland appears less than predicted by the model based on Norwegian inventory, whereas pine and birch grow faster. The original model parameters indicated negative growth rates at large stand basal areas. Refitting of model parameters corrected the deficiencies. Stand age effect was included but found to be weak. Site fertility index fitted to diameter growth observations become higher on dryish sites, compared to mesic sites. Such finding agreed with greater stand basal area increment rate on the dryish sites. Reasons for the apparent site fertility discrepancy are discussed.

Keywords: *Picea abies, Pinus sylvestris, Betula pendula, Betula pubescens*

Introduction

The simplest way to describe or predict forest growth is through growth or yield tables, yield here referring to accumulated growth [1, 2]. Such tables may or may not be produced using growth or yield equations, equations being more widely applicable than tables alone [3, 4]. Applicability may be further enhanced by including some kind of a description of stand structure [2, 5, 6]. A further refinement would be the inclusion of properties of single trees [7, 8, 9, 10], and possibly even relationships between single trees [11, 12, 13].

Even if parameters describing forest stand structure often are included in growth models, a growth model generally is one of the essential ingredients in any dynamic demographic model of forest stand structure [2, 14, 15, 16, 17]. Consequently, it is possible to evaluate growth models on the basis of their implications on forest stand structure. The forest stand structure, in turn, is most unambiguously discussed in a stationary (or equilibrium) state, where all time derivatives approach zero. Even if diameter growth models seldom are designed to describe stationary states, their asymptotic behavior may reveal their logical structure; one can safely state that models eventually predicting infinite timber stock in a finite space are logically inconsistent.

One possible implementation of a dynamic demographic model is a matrix containing the appearance frequency of trees in discrete size classes of different tree species [18, 19, 20, 21, 22, 23, 24, 25]. Within a time step, a transition matrix transfers some trees to another class of larger diameter, another transition matrix removes dying trees. Interaction with the frequency matrix may occur in terms of Hadamard multiplication. Using index notation, the change in appearance frequency along with a time step can be written as

$$\Delta n_{pq} = r_{pq} + \left[1 - m_{(p-1)q}\right] id_{(p-1)q} n_{(p-1)q} - \left[\left(1 - m_{pq}\right) id_{pq} + m_{pq}\right] n_{pq} \quad (\text{no sum}) \quad (1),$$

where p refers to diameter classes, q to tree species, n_{pq} is appearance frequency, r_{pq} is recruitment frequency, id_{pq} is growth transition probability, and m_{pq} is mortality probability. However, all recruitment appears into the lowest diameter class and thus the only nonzero recruitment terms are r_{1q} . On the other hand, n_{0q} and id_{0q} are indefinite. Then, stationarity conditions for the system become

$$\begin{aligned} \Delta n_{1q} &= r_{1q} - \left[\left(1 - m_{1q}\right) id_{1q} + m_{1q}\right] n_{1q} = 0 \quad (\text{no sum}) \\ \Delta n_{pq} &= \left(1 - m_{(p-1)q}\right) id_{(p-1)q} n_{(p-1)q} - \left[\left(1 - m_{pq}\right) id_{pq} + m_{pq}\right] n_{pq} = 0 \quad \text{for } p > 1 \quad (\text{no sum}) \end{aligned} \quad (2),$$

Let us discuss the asymptotic behavior of a few dynamic demographic models at the limit of stationary state.

Firstly, a spruce stand in the stationary state, according to the model by Bollandsås et al. [22] is shown in Fig. 1. It is found that there is a unimodal distribution of tree basal area below the diameter of 700 mm, and then there are barely any trees larger than that. There is a computational instability only at the end of the data.

Then, a Mediterranean Scots pine stand in the stationary state, according to the model by Trasobares et al. [20] is also shown in Fig. 1. A unimodal distribution of tree size-class basal area appears. Within the growth model by Trasobares et al. [20], the estimate of the mortality does not vanish along with tree size. The estimated diameter growth declines along with tree size but interacts with mortality to combine a mode value that corresponds to the empirical observations [20].

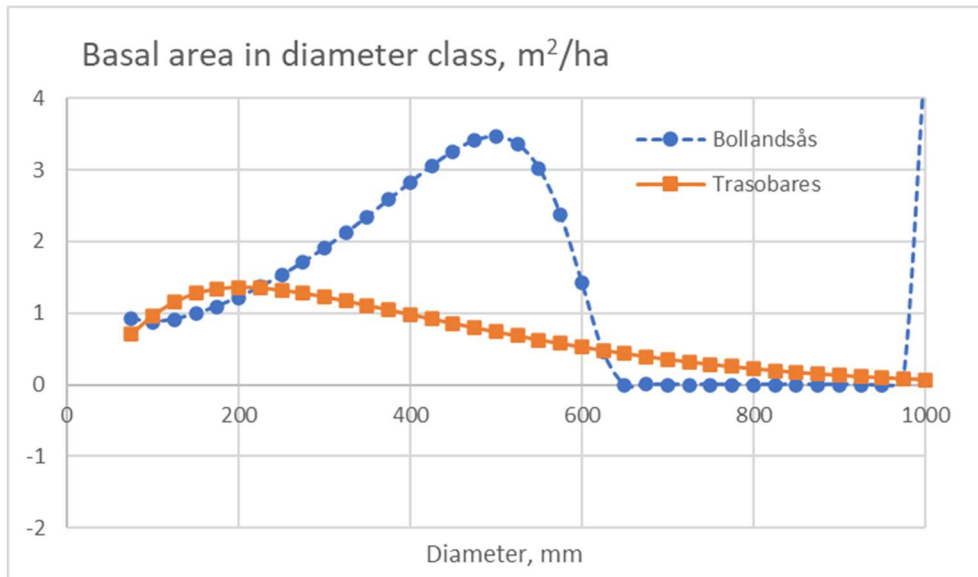


Fig. 1. Stand basal area in 25 mm diameter classes in the stationary state according to Eq. (2), using the Norway spruce growth model of Bollandsås et al. [22], and Mediterranean Scots pine growth model of Trasobares et al. [20].

Secondly, a spruce stand in the stationary state, according to the model by Pukkala et al. [23] is shown in Fig. 2. It is found that there is no unimodal distribution of tree basal area below the diameter of 700 mm, and then, a very large number of large trees appears. The divergence of the size distribution obviously is since along with tree diameter, both mortality and diameter growth vanish, mortality vanishing faster. The slowly vanishing diameter increment rate then accumulates trees into the large end of the distribution.

A Maritime pine stand in the stationary state, according to the model by Rosa et al. [25] is also shown in Fig. 2. It is found that there again is no unimodal distribution of tree size-class basal area. Within the growth model by Rosa et al. [25], the estimate of the mortality vanishes but the estimate of the diameter growth rate increases continuously as a function of tree size. Then, the stem count in any size class in the stationary state is reduced according to Eq. (2), but slowly enough to induce a continuous increment of size-class basal area as a function of increasing tree size (Fig. 2). A similar phenomenon is found in the study of Trasobares et al. [21]: estimated *Pinus halepensis* diameter growth rate continuously increases with diameter, apparently resulting as infinite timber stock to accumulate in finite space (Fig. 2).

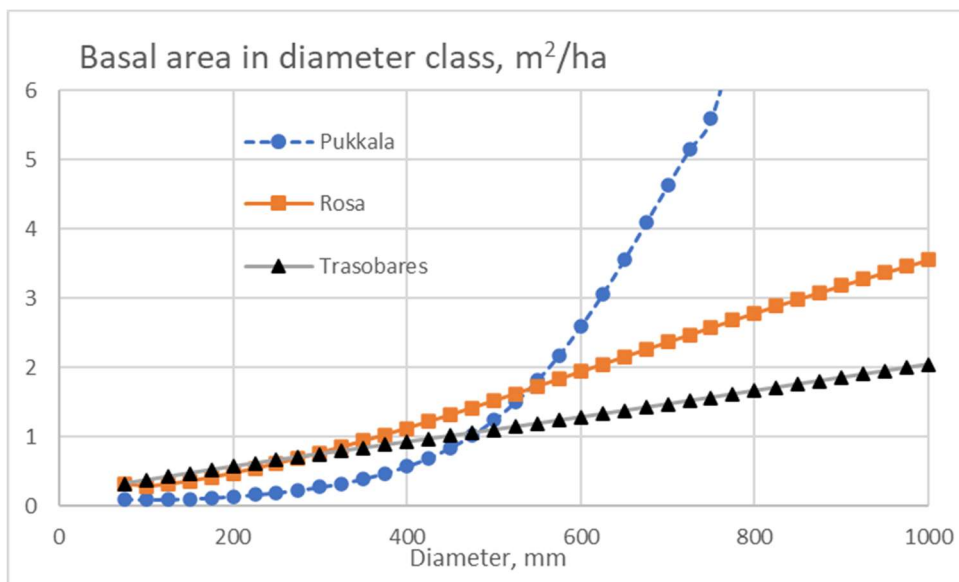


Fig. 2. Stand basal area in 25 mm diameter classes in the stationary state according to Eq. (2), using the Norway spruce growth model of Pukkala et al. [23], Maritime pine growth model of Rosa et al. [25], and *Pinus halepensis* growth model of Trasobares et al. [21].

Obviously, infinite timber stocks cannot appear in finite space. Correspondingly, the growth models appearing in Fig. 2 possibly should not be utilized in further developments. The growth models appearing in Fig. 1 do not suffer from such deficiency. The present data being collected from boreal sites, we will here adopt the model by Bollandsås et al. [22] for further investigation.

Materials and Methods

Diameter growth of rate of 10849 trees from South-Central Finland, close to the University of Helsinki research station, was determined with measurements repeated with intervals of 3 to 6 years. 2846 of the trees were of pine species (*Pinus silvestris*), 7011 of spruce (*Picea abies*), 1248 of silver birch (*Betula pendula*), and 744 of downy birch (*Betula pubescens*). 1660 trees

were measured from 24 measurement plots on dryish forest sites, 9716 trees from 75 plots on mesic sites, and 737 from six plots on herb-rich sites.

For any tree, the diameter growth rate was predicted using the growth function of Bollandsås et al. [22] as

$$I_{ijk} = a_{jk} b_{ik} / \Delta t \quad (3),$$

where b_{ik} is one of eight properties k characterizing an individual tree i , and a_{jk} refers to one of eight coefficients k , specific to tree species j , and Δt is the forward duration of the prediction period.

The eight properties used to predict diameter growth rate are as shown in Table 1. The 32 species-specific model coefficients appearing in Eq. (3), in their original form [22], are given in Table 2. The number of observations, and the expected values of tree diameter and observed diameter growth rate are shown in Table 3.

Table 1. Eight factors contributing to Eq. (3).

b1	Unity (constant)
b2	Breast-height diameter [mm]
b3	Breast-height diameter squared [(mm) ²]
b4	Breast-height diameter in cubic [(mm) ³]
b5	Basal area of larger trees [m ² /ha]
b6	Site Index [m]
b7	Basal area of stand [m ² /ha]
b8	Latitude [degrees]

Table 2. Species-specific coefficients contributing to Eq. (3).

	Pine	Spruce	Silver birch	Downy birch
a1	25.542600	17.839300	11.808400	11.808400
a2	0.025090	0.047620	0.000000	0.000000
a3	-0.000057	-0.000116	0.000096	0.000096
a4*10 ⁴	0.000000	0.000000	-0.000959	-0.000959
a5	-0.216220	-0.341160	0.000000	0.000000
a6	0.698140	0.906040	0.518500	0.518500
a7	-0.123180	-0.024140	-0.151760	-0.151760
a8	-0.336260	-0.267810	-0.160520	-0.160520

The expected value of predicted diameter growth, for any tree species and site fertility, is also shown in Table 3. Site fertility index as given by Bollandsås et al. [22], fitted separately for any of the three site fertility classes by minimizing the squared error between the observed and predicted diameter growth rate of any tree within the fertility class. Table 3 also shows the expected value of basal area per hectare and the growth rate of basal area, as well as stem count

of trees of at least 100 mm diameter, and the stand age of measurement plots within any site fertility class.

Table 3. Expected values of observations, as well as model predictions.

	Count	Diameter [mm]	Diameter growth [mm/a]	Predicted diameter growth [mm/a]	Fitted Site Index	Basal Area [m ² /ha]	Growth rate of BA [m ² /(ha*a)]	Stem count/ha (100mm +)	Age [a]
Dryish, <i>Pinus silvestris</i>	906	191	2.31	2.42	16.9	28.44	0.64	793	66
Dryish, <i>Picea abies</i>	539	137	2.45	2.50					
Dryish, <i>Betula pendula</i>	95	149	2.82	1.83					
Dryish, <i>Betula pubescens</i>	92	97	2.42	1.65					
Mesic, <i>Pinus silvestris</i>	1799	229	2.42	2.12	15.2	30.69	0.51	747	73
Mesic, <i>Picea abies</i>	6163	177	2.00	2.10					
Mesic, <i>Betula pendula</i>	1103	188	1.92	1.74					
Mesic, <i>Betula pubescens</i>	461	133	1.56	1.45					
Herb-rich, <i>Pinus silvestris</i>	141	216	3.84	3.27	18.1	20.93	0.71	787	38
Herb-rich, <i>Picea abies</i>	309	138	2.27	2.90					
Herb-rich, <i>Betula pendula</i>	50	111	3.45	1.70					
Herb-rich, <i>Betula pubescens</i>	191	135	2.73	1.94					

An interesting feature in Table 3 is that the fitted site index on dryish sites is greater than the fitted site index on mesic sites. Also, the expected (area-weighted) site-level increment rate of the basal area is greater on the dryish sites.

One possible candidate for the high growth rates on the dryish sites is the distribution of tree species: as the diameter growth rate is modeled as a linear function of the site index, the corresponding coefficients do vary by tree species. Even if the site fertility index characterizes the site independently of tree species, the suitability of the original model coefficients relating site fertility to diameter growth rate can be investigated by fitting the site index separately for any tree species.

An apparent site index fitted for any tree species separately is shown in Table 4. It is found that in all cases the best fit of site index for the growth of spruce trees is less than the average. The growth of birch trees is generally greater than the average, whereas the growth of pine trees does not differ much from the average. The findings indicate that, in relative terms, Norway spruce trees grow better in Norway [22], and birch trees grow better in Finland. Consequently, the model parameters, with respect to site fertility, have to be adjusted.

Table 4. Apparent site indices providing the least squared errors.

			Silver	Downy		Arithmetic	Abundance-weighted
	Pine	Spruce	birch	birch		average	average
Dryish	16.2	16.6	26.5	24.6		21.0	17.5
Mesic	17.4	14.7	16.9	16.3		16.3	15.5
Herb-rich	22.0	14.3	34.8	25.4		24.1	20.2

Technically, the adjustment of the site fertility coefficients is as follows. A common site fertility index for the mesic sites was first recovered as the best fit appearing in Table 3. Then, the linear model coefficient describing the site fertility effect on the diameter growth rate is fitted for the minimum of squared model error, separately for any tree species within the mesic sites. The site fertility coefficient is fitted interactively with the constant term of Eq. (3). After

fixing the site fertility coefficients, site fertility indices were refitted for any of the three site fertility classes by minimizing the sum of squared errors. After fixing the site fertility indices, all data were combined, and the site fertility coefficients for any of the tree species were refitted, for the verification of the success of the tree species adjustment.

Another issue that apparently requires attention is that model predictions for the diameter increment rate yielded negative values at the high basal area and basal area of larger trees. The model parameters were correspondingly adjusted, the two linear model parameters interactively with the constant term, for minimum squared prediction error. Further, an attempt was made to adjust the linear term relating to tree diameter.

A methodological question is, how the effect of the model parameters on model results should be illustrated. This is not completely straightforward since seven observables appearing in Table 1 contribute to any result simultaneously. An instructive solution is the use of mean-field approximations. One contributor appearing in Table 1 at a time is selected as the independent variable. Then, the expected value of any other contributor for any relevant value interval of the independent variable is clarified. Finally, the expected values are used in the computation of the model result for any value interval of the independent variable.

Results

Adjusting the site fertility coefficient a_6 for any of the three tree species, along with the terms a_1 , a_2 , a_5 , a_6 , and a_7 , resulted in modified diameter increment rate prediction coefficients according to Table 5.

Table 5. The 32 species-specific model coefficients appearing in Eq. (3), adjusted by least-squares fitting.

	Pine	Spruce	Silver birch	Downy birch
a1	23.800000	14.300000	13.700000	16.500000
a2	0.025090	0.047620	0.000000	0.000000
a3	-0.000057	-0.000116	0.000096	0.000096
a4	0.000000	0.000000	-0.000959	-0.000959
a5	-0.159000	-0.198000	-0.156000	-0.127000
a6	0.800000	0.870000	0.575000	0.555000
a7	-0.105000	-0.010000	-0.099000	-0.182000
a8	-0.336260	-0.267810	-0.160520	-0.160520

Consequently, the model results appearing in Table 3 were modified as shown in Table 6. There now is a closer agreement between the expected values of predictions and observations. However, the fitted site index for the dryish sites still is greater than that for the mesic sites, in accordance with the basal area growth rate per area unit being greater on the dryish sites.

Table 6. Expected values of observations, as well as model predictions, after adjusting the model coefficients as shown in Table 5.

	Count	Diameter [mm]	Diameter growth [mm/a]	redicted diamet growth [mm/a]	Fitted Site Index	Basal Area [m ² /ha]	Growth rate of BA [m ² /(ha*a)]	Stem count/ha (100mm +)	Age [a]
Dryish, Pinus silvestris	906	191	2.31	2.57	16.2	28.44	0.64	793	66
Dryish, Picea abies	539	137	2.45	2.22					
Dryish, Betula pendula	95	149	2.82	2.07					
Dryish, Betula pubescens	92	97	2.42	2.03					
Mesic, Pinus silvestris	1799	229	2.42	2.32	15.0	30.69	0.51	747	73
Mesic, Picea abies	6163	177	2.00	1.99					
Mesic, Betula pendula	1103	188	1.92	2.03					
Mesic, Betula pubescens	461	133	1.56	1.77					
Herb-rich, Pinus silvestris	141	216	3.84	3.42	18.1	20.93	0.71	787	38
Herb-rich, Picea abies	309	138	2.27	2.70					
Herb-rich, Betula pendula	50	111	3.45	1.86					
Herb-rich, Betula pubescens	191	135	2.73	2.43					

Again, site fertility does not vary by tree species, but eventual differences in species-specific growth rate, in comparison to model predictions, can be investigated by fitting apparent species-specific site indices. After fitting the coefficients as explained above, the apparent site indices are shown in Table 7. It is found that the fitting has leveled off most of the variation that appeared in Table 4.

Table 7. Apparent site indices providing the least squared errors, after adjusting the model coefficients as shown in Table 5.

			Silver	Downy	Arithmetic	Abundancy- weighed
	Pine	Spruce	birch	birch	average	average
Dryish	14.5	17.5	22.6	19.7	18.6	16.3
Mesic	15.5	15.1	13.9	13.1	14.4	14.9
Herb- rich	20.6	15.4	31.7	20.8	22.1	18.9

Figure 3 shows the effect of tree diameter on the diameter increment rate, for original model parameters and modified model parameters, as a mean-field approximation. It is found that the modified parameters result in lower growth of spruce trees, and higher growth of other tree species, in concert with Table 4. While other tree species show the greatest diameter growth at diameters between 200 and 300 mm, large, dominant silver birch trees grow fastest. The latter model finding was positively verified from the original measurements.

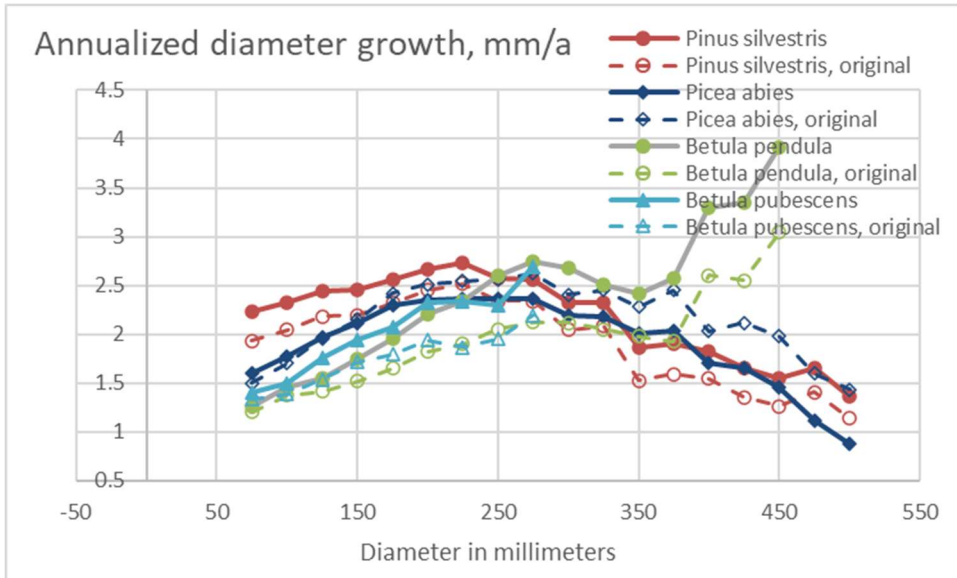


Fig. 3. Mean-field approximations for the effect of tree diameter on diameter increment rate, for original model parameters (dashed lines) and modified model parameters (solid lines).

Figure 4 shows the effect of stand basal area on the diameter increment rate, for original model parameters and modified model parameters, as mean-field approximations. Again, the modified parameters result in lower growth of spruce trees, and higher growth of other tree species, in concert with Table 4. However, in the case of spruce and pine trees, the modified model indicates a smaller diameter growth-reducing effect of the basal area with the modified parameters. Consequently, predicted negative growth rates, appearing while using the original parameters, are avoided. In the case of downy birch trees, the modified parameters result in a stronger growth-reducing effect of basal area.

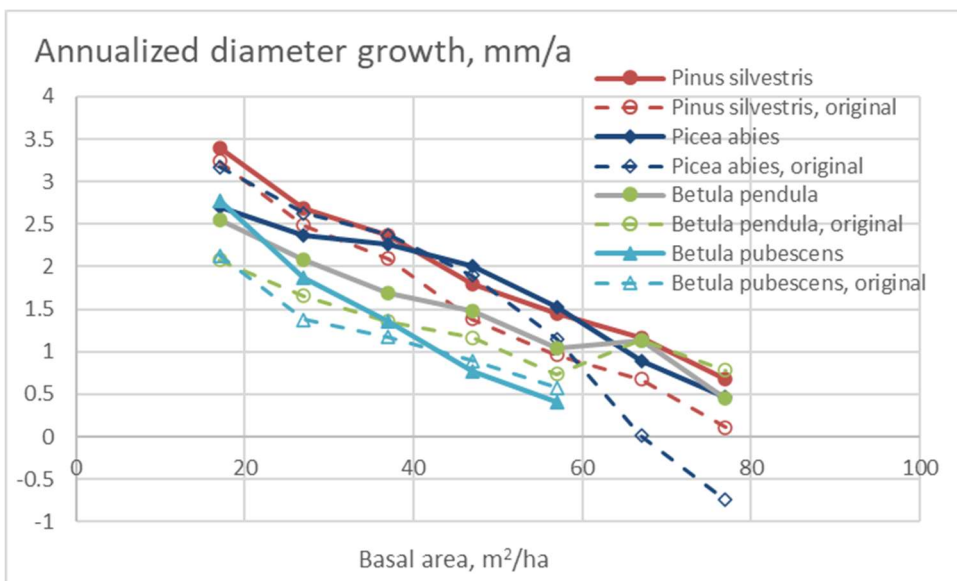


Fig. 4. Mean-field approximations for the effect of basal area on diameter increment rate, for original model parameters (dashed lines) and modified model parameters (solid lines).

Figure 5 shows the effect of the basal area of larger trees on any stand on diameter increment rate, for original model parameters and modified model parameters, as mean-field approximations. Again, the modified parameters result in higher growth of other tree species but spruce, in concert with Table 4. The modified parameters result in lower growth rate of spruce trees, provided the basal area of larger trees is at most 23 m²/ha. In the case of spruce and pine trees, the modified model indicates a smaller diameter growth-reducing effect of the basal area of larger trees with the modified parameters. Consequently, the predicted negativity of growth rates, appearing while using the original parameters, is reduced. In the case of birch trees, the modified parameters result in a stronger growth-reducing effect of the basal area of larger trees. It is further worth noting that at high basal area of larger trees, the diameter increment rate of spruce trees is bigger than that of pine trees.

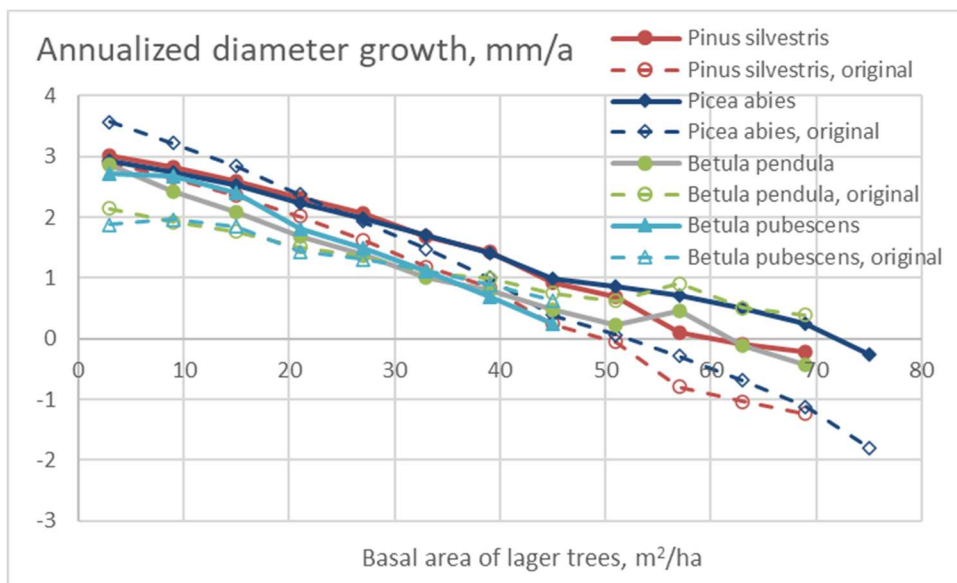


Fig. 5. Mean-field approximations for the effect of basal area of larger trees on diameter increment rate, for original model parameters (dashed lines) and modified model parameters (solid lines).

Figure 6 shows the effect of the site index on diameter increment rate, for original model parameters and modified model parameters, as mean-field approximations. Again, the modified parameters result in higher growth of other tree species but Norway spruce, and lower growth in the case of spruce, in concert with Table 4. The diameter increment rate of silver birch is insensitive to the site index [cf. 26,27], whereas with other species, larger site index indicates a greater diameter increment rate. The diameter increment rate of pine trunks is the greatest, followed by Norway spruce, and then the birch species.

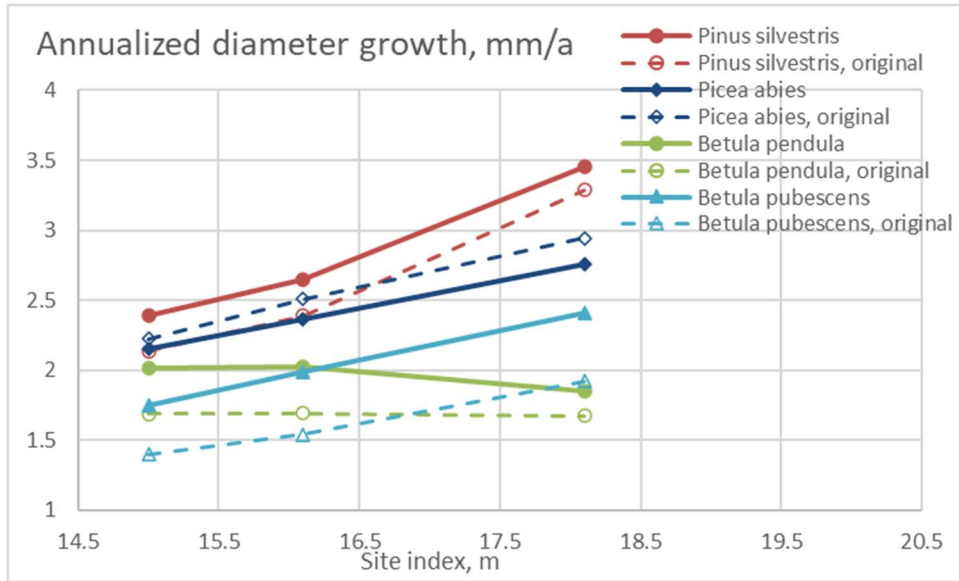


Fig. 6. Mean-field approximations for the effect of site index on diameter increment rate, for original model parameters (dashed lines) and modified model parameters (solid lines).

Discussion

The original growth function of Bollandsås et al. [22] did not contain stand age, neither tree age, as an independent variable. It is however interesting whether stand age estimates would contribute to diameter increment rates of trees. An attempt to fit a ninth model parameter, multiplying the estimated age of any stand, is reported in Table 8. It is found that the sign of the age effect varies by tree species, and the age effect is not very strong.

Table 8. The 36 species-specific model coefficients appearing in Eq. (3) amended by stand age as an independent variable, adjusted by least-squares fitting.

	Pine	Spruce	Silver birch	Downy birch
a1	23.800000	13.800000	13.200000	16.600000
a2	0.025090	0.047620	0.000000	0.000000
a3	-0.000057	-0.000116	0.000096	0.000096
a4*10 ⁴	0.000000	0.000000	-0.000959	-0.000959
a5	-0.159000	-0.198000	-0.156000	-0.127000
a6	0.800000	0.870000	0.575000	0.555000
a7	-0.105000	-0.010000	-0.099000	-0.182000
a8	-0.336260	-0.267810	-0.160520	-0.160520
a9	-0.006000	0.0100	0.011000	-0.003000

Figure 7 shows the effect of stand age on diameter increment rate, for original model parameters and modified model parameters, as mean-field approximations. Again, the modified parameters result in higher growth of other tree species but Norway spruce, and lower growth in the case of spruce, in concert with Table 4. In concert with Fig. 4, the modified parameters remove the negative predictions of diameter increment rate.

It is worth noting that the original parameters do not contain any nonzero coefficient for stand age. Correspondingly, within the original parameter set, the stand age contributes to the diameter increment rate only through the other parameters (Table 1) being affected by stand age within the mean-field approximation.

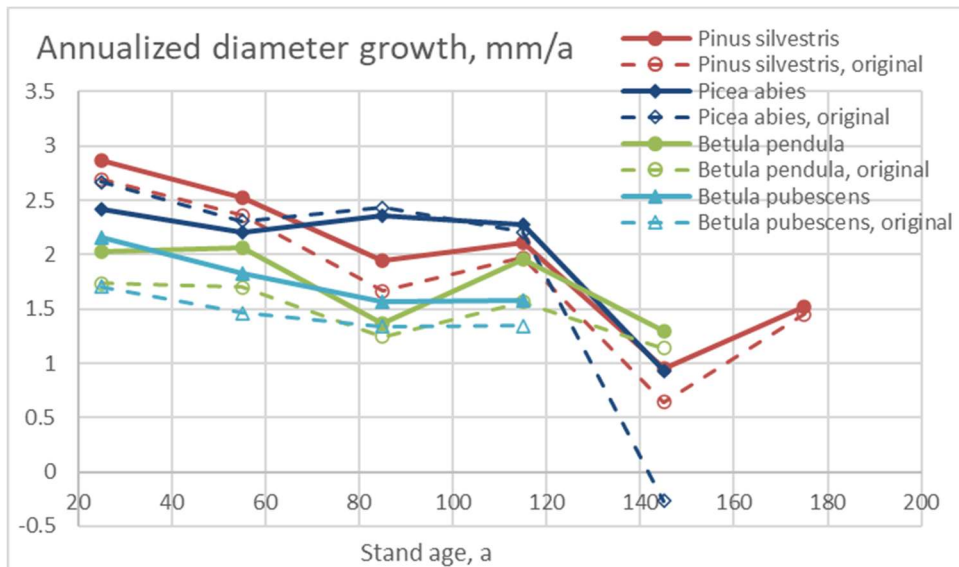


Fig. 7. Mean-field approximations for the effect of stand age on diameter increment rate, for original model parameters (dashed lines) and modified model parameters (solid lines).

As the parameters of the diameter increment rate model have been adjusted for the Finnish dataset as shown in Table 5, instead of the original values in Table 2, it would be of interest to discuss how the steady-state solution for the basal area distribution (Figure 1) would be affected. However, the outcome in Fig. 1 does not only depend on the diameter increment rate, but also on model parameters explaining mortality and recruitment of trees into the smallest diameter class. The latter parameters remain subject to forthcoming studies, and thus we resist the temptation of redrawing Fig. 1 at this stage.

As Figures 3 to 7 reflect modeled tree diameter growth, it is of interest to discuss the relation of tree diameter growth to forest growth. Obviously, there is no straightforward relation. Basal area growth rate of a tree can be simply given in terms of tree size times diameter increment rate, but the forest growth per hectare depends on stem count, tree species distribution, tree size distribution within any species, and so on.

On the basis of the present data, it is possible to investigate the effect of stand-level parameters on forest site basal area growth. Figure 8 shows the relationship between stand basal area and basal area growth rate. It is found that within the mesic sites, the basal area increment rate slightly decreases with increasing basal area. In the case of dryish and herb-rich sites, large basal areas do not appear in this dataset. In the case of herb-rich sites, the basal area increment rate apparently increases with basal area.

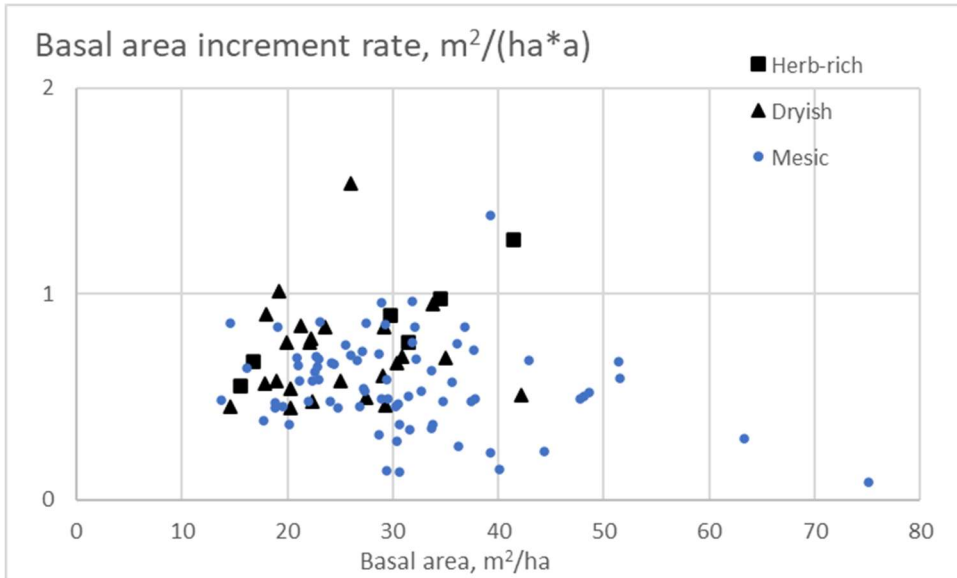


Fig. 8. Relationship between stand basal area and basal area growth rate for the three different site fertility classes.

Figure 9 shows the relationship between stand age and basal area growth rate. It is found that within the mesic sites, the basal area increment rate slightly decreases with increasing stand age. In the present dataset, the herb-rich sites are all young, as well as most of the dryish stands.

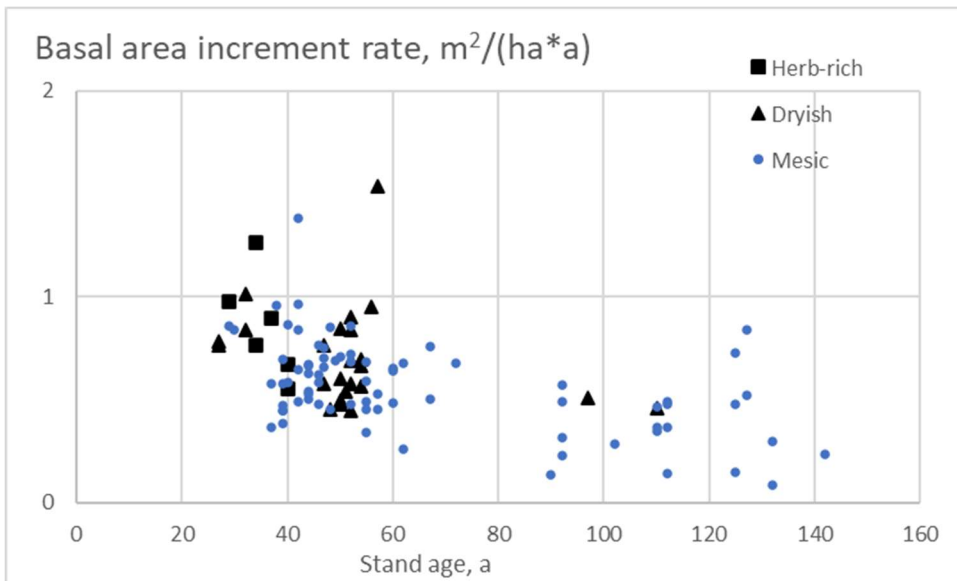


Fig. 9. Relationship between stand age and basal stand area growth rate for the three different site fertility classes.

Figure 10 shows the relationship between the number of trees of at least 100 mm diameter per area unit and basal area growth rate. It is found that the basal area increment rate increases with increasing stem count, being greater on the dryish sites than on the mesic sites.

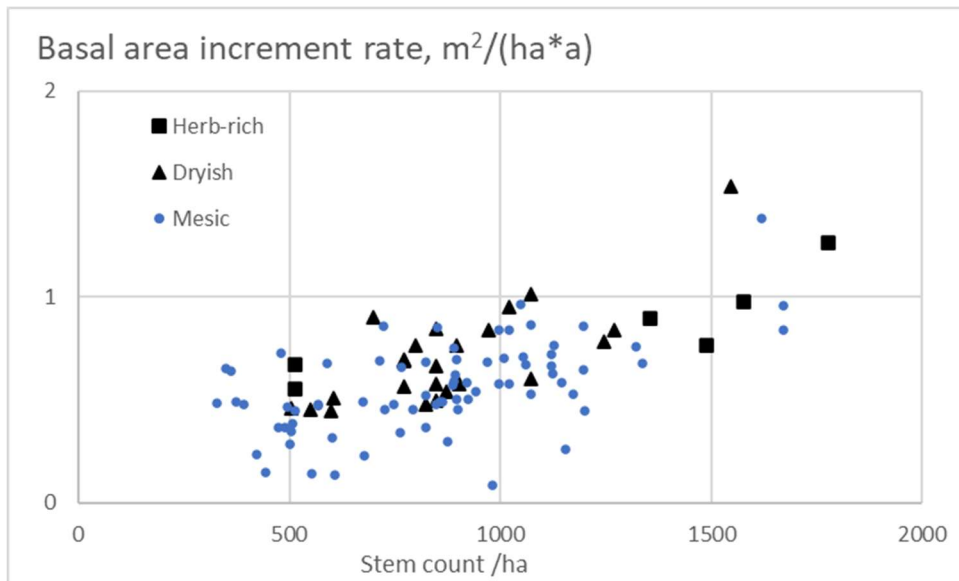


Fig. 10. Relationship between stem count and basal stand area growth rate for the three different site fertility classes.

Figure 11 shows the relationship between the site fertility index and the basal area growth rate. It is found that the basal area increment rate increases with increasing site fertility index, even if the site index is greater on the dryish sites than on the mesic sites.

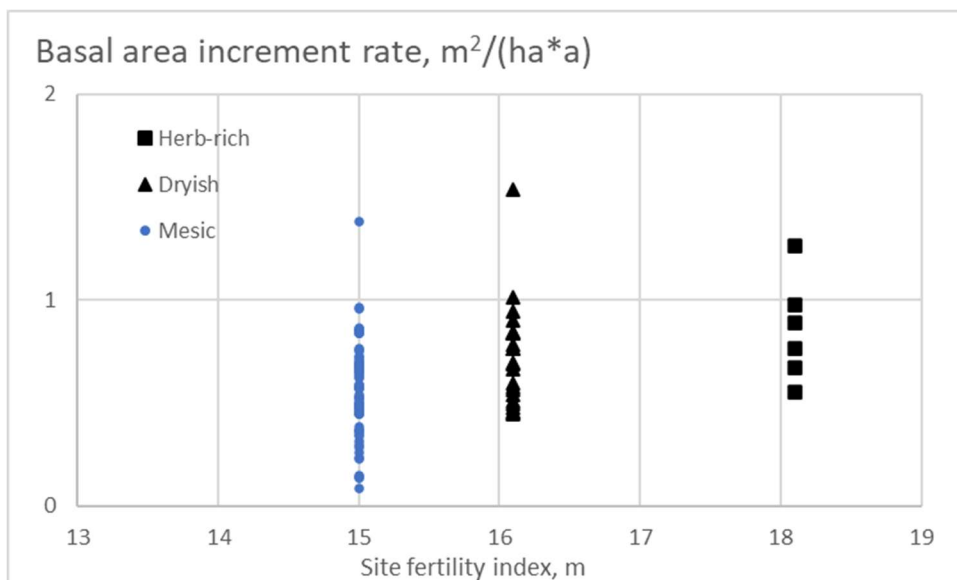


Fig. 11. Relationship between site fertility index and basal stand area growth rate for the three different site fertility classes.

It is worth discussing why the dryish sites appear more fertile and more productive than the mesic sites. Firstly, the tree species distribution differs (Table 3), and in the present data, the growth rate of pine trees is greater than that of spruce trees (Figs. 3, 4 and 6). Secondly, the dryish stands of this data are of younger age, and smaller basal area (Figures 8 and 9). Thirdly, it is possible that the actual fertility does not differ too much between the dryish and the mesic sites; the visual judgement regarding the fertility class of any stand may have been affected by the tree species distribution (Table 3).

Differences definitely appear between the original model [22] and the model refitted using the present dataset. Spruce trees grow slower, pine and birch faster (in relative terms) in Finland. The authors are not aware of previous investigations reporting such difference. Figures 3 to 7 indicate that at young age, pine diameter growth exceeds that of spruce, which agrees with published data [28, 29, 30].

Appearance of negative growth predictions when using the original model parameters partially is explained by the fact that large basal areas appearing in the present dataset did not occur in the Norwegian dataset [22]. It is however worth noting that the most wooded and oldest stands appearing in the present dataset represent conservation sites and would not frequently appear in commercial forestry.

Even if the differences between the datasets and the corresponding model results from the two countries are clearly observable, it is worth noting that there is much variation in the experimental observations. One of the reasons for the variation is that repeated measurements of diameter contain more random error than growth ring analysis [31, 18]. The model results represent expected values of observables, and thus can be used in management considerations, but do not predict the development of individual trees or stands precisely. Management considerations shall differ with different model parameters. Many considerations may be functional regardless of the parameter set used. On the other hand, the relative benefit of Pine (*Pinus silvestris*) trees in the local dataset may affect some applications.

Acknowledgement

This study was partially financed by Niemi Foundation.

Drs. Ilkka Korpela and Aarne Hovi are gratefully acknowledged for their contributions to Data Acquisition.

References

1. Spurr, S.H. (1952). Forest Inventory. Ronald, N.Y. 476 p.
2. Reineke, L.H. (1927). A modification of Bruce's method of preparing timber yield tables. J. Agric. Res. 35, 843–856.
3. Bertalanffy, L.V. (1941). Untersuchungen über die Gesetzlichkeit des Wachstums. VII. Stoffwechselltypen und Wachstumstypen. Biol. Zbl. 61, 510–532.
4. Vuokila, Y. (1965). Functions for variable density yield tables of pine based on temporary sample plots. Commun. Inst. For. Fenn. 60(4):1–86.
5. García, O. (2011). The state-space approach in growth modelling. Canadian Journal of Forest Research. 24(9), 1894-1903. <https://doi.org/10.1139/x94-244>.
6. Andreassen, K. & Øyen, B. (2014). Comparison of selected Nordic stand growth models for Norway spruce, Scots pine and birch. Forestry Studies, 55(1), 46-59. doi:10.2478/v10132-011-0101-y
7. Stage, A. R. (1973). Prognosis model for stand development. USDA For. Serv., Res. Pap. INT-137. 32 p.

8. Leary, R. A. (1979). Design. In: A generalized forest growth projection system applied to the lake states region. USDA For. Serv., Gen. Tech. Rep. NC-49, pp. 5–15.
9. Daniels, R. F. & Burkhardt, H.E. (1988). An integrated system of forest stand models. *For. Ecol. Manage.* 23, 159–177.
10. Buongiorno, J., Peyron, J. L., Houllier, F. & Bruciamacchie, M. (1995). Growth and management of mixed-species, uneven-aged forests in the French Jura: Implications for the economic returns and tree diversity. *Forest Science* 41, 397–429.
11. Lemmon, P. E. & Schumacher, F.X. (1962). Stocking density around ponderosa pine trees. *For. Sci.* 8, 397–402.
12. Daniels, R. F., Burkhardt, H. E. & Clason, T. R. (1986). A comparison of competition measures for predicting growth of loblolly pine trees. *Can. J. For. Res.* 16, 1230–1237.
13. Nance, W. L., Grissom, J. E. & Smith, W. R. (1988). A new competition index based on weighted and constrained area potentially available. In A.R. Ek, S.R. Shifley and T.E. Burk (eds) *Forest Growth Modelling and Prediction. Proc. IUFRO Conf., 23–27 Aug. 1987, Minneapolis, MN. USDA For. Serv., Gen. Tech. Rep. NC-120, pp. 134–142.*
14. Schütz, J.-P. (1997). Conditions of Equilibrium in fully irregular, uneven-aged forests: The state-of-the-art in European plenter forests September 1997 Conference: IUFRO Interdisciplinary Uneven-aged management symposium At: Oregon State University, Corvallis, USA
15. Schütz, J.-P. (2006). Modelling the demographic sustainability of pure beech plenter forests in Eastern Germany. *Annals of Forest Science* 63(1).
16. Brzeziecki, B., Pommerening, A., Miścicki, S., Drozdowski, S. and Żybura, H. (2016), A common lack of demographic equilibrium among tree species in Białowieża National Park (NE Poland): evidence from long-term plots. *J Veg Sci* 27, 460–469. doi:10.1111/jvs.12369
17. Olofsson, L., Langvall, O. & Pommerening, A. (2023). Norway Spruce (*Picea abies* (L.) H. Karst.) selection forests at Siljansfors in Central Sweden. *Trees, Forests and People* 12, 100392. <https://doi.org/10.1016/j.tfp.2023.100392>.
18. Monserud, R. A. & Sterba, H. (1996). A basal area increment model for individual trees growing in even- and uneven-aged forest stands in Austria, *Forest Ecology and Management* 80(1-3), 57-80. [https://doi.org/10.1016/0378-1127\(95\)03638-5](https://doi.org/10.1016/0378-1127(95)03638-5).
19. Palahi, M., Pukkala, T., Miina, J. & Montero, G. (2003). Individual-tree growth and mortality models for Scots pine (*Pinus sylvestris* L.) in north-east Spain. *Annals of Forest Science* 60(1), 1-10.
20. TRASOBARES, A., PUKKALA, T. & MIINA J. (2004). Growth and yield model for uneven-aged mixtures of *Pinus sylvestris* L. and *Pinus nigra* Arn. in Catalonia, north-east Spain. *Ann. For. Sci.* 61, 9–24.
21. Trasobares, A., Tome, M. & Miina, J. (2004). Growth and yield model for *Pinus halepensis* Mill in Catalonia, north-east Spain. *Forest Ecology and Management* 203, 49–62.
22. Bollandsås, O. M., Buongiorno J. & Gobakken, T. (2008). Predicting the growth of stands of trees of mixed species and size: a matrix model for Norway. *Scand J For Res* 23, 167–178.
23. Pukkala, T., Lähde, E. & Laiho, O. (2009). Growth and yield models for uneven-sized forest stands in Finland. *For. Ecol. Manage.* 258(3), 207–216. doi:10.1016/j.foreco.2009.03.052.
24. Pukkala, T., Lähde, E. & Laiho, O. (2010). Optimizing the structure and management of uneven-sized stands in Finland. *Forestry*, 83(2), 129–142. doi:10.1093/forestry/cpp037.
25. Rosa, R., Soares, P. & Tomé M. (2018). Evaluating the Economic Potential of Uneven-aged Maritime Pine Forests. *Ecological Economics* 143, 210-217.
26. Raulo, J. (1977). Development of dominant trees in *Betula pendula* Roth and *Betula pubescens* Ehrh. plantations. Seloste: Viljeltyjen raudus- ja hieskoivikoidenvaltapuiden kehitys. *Communicationes Instituti Forestalis Fenniae* 90(4).

27. Oikarinen, M. (1983). Etelä-Suomen viljeltyjen raudus-koivikoiden kasvatusmallit. Summary: Growth and yield models for silver birch (*Betula pendula*) plantations in southern Finland. *Communications Instituti Forestalis Fenniae* 113.
28. Eklund, B. (1954). Årsringsbreddens klimatiskt betingande variation hos tall och gran inom norra Sverige åren 1900—1944. Summary: Variations in the widths of the annual rings in pine and spruce due to climate conditions in Northern Sweden during the years 1900—1944. *Meddelanden från statens skogsforskningsinstitut* 44.8.
29. Mikola, P. (1950). Puiden kasvun vaihtelusta ja niiden merkityksestä kasvututkimuksissa. *Communications Instituti Forestalis Fenniae* [838] 38.5, 1—125.
30. Mielikäinen K., Timonen M. & Nöjd P. (1996). Männyn ja kuusen kasvun vaihtelu Suomessa 1964–1993. *Metsätieteen aikakauskirja* 1996(4), 309-320.
<https://doi.org/10.14214/ma.6728>
31. Wykoff, W. R. (1990). A Basal Area Increment Model for Individual Conifers in the Northern Rocky Mountains. *Forest Science* 36(4), 1077–1104.
<https://doi.org/10.1093/forestscience/36.4.1077>